IET Science, Measurement & Technology

Research Article

Radio interference excitation function of conductor bundles based on cage test results and comparison with long-term data

ISSN 1751-8822
Received on 27th July 2014
Accepted on 7th November 2014
doi: 10.1049/iet-smt.2014.0224
www.ietdl.org

Wang-ling He[1] ✉, *Jun-jia He*[1], *Bao-quan Wan*[2], *Yu-chao Chen*[2], *Chun-ming Pei*[2], *Jian-gong Zhang*[1,2], *Jin Zhang*[1,3]

[1]*School of Electrical and Electronic Engineering, Huazhong University of Science and Technology, Wuhan, People's Republic of China*
[2]*AC Electromagnetic Environmental Department, China Electric Power Research Institute, Wuhan, People's Republic of China*
[3]*Quality Inspection and Test Center for Electric Equipment of Power Industry, China Electric Power Institute, Wuhan, People's Republic of China*
✉ *E-mail: wanglinghe88@gmail.com*

Abstract: A reasonable excitation function is vital to make a precise evaluation about the radio interference (RI) level of ultra-high-voltage (UHV) AC power lines. To obtain this function, a large number of RI measurements in heavy rain condition were done using different conductor bundles in a corona cage. Then, the excitation function in heavy rain condition was obtained by least-square fitting these measured values. After that, the validity of this function was verified with the statistical data measured from the Hubei long-term station, which is located under the operating 1000 kV Jindongnan–Nanyang–Jingmen UHV AC transmission lines. It turns out that the deviation between the prediction and the long-term average value is 1.1 dB in heavy rain condition, and 1.3 dB in fair weather condition. In addition, the long-term data measured in Hubei Station show that the conversion laws of RI at different weather conditions in International Special Committee on Radio Interference (CISPR)18 are also applicable to 1000 kV UHV transmission lines.

1 Introduction

The ultra-high-voltage (UHV) AC transmission lines are indispensable to the development of electric power transmission in China nowadays. With the increase in voltage, however, the radio interference (RI) field strength becomes more serious [1]. Therefore a precise estimation and effective control of RI level of UHV AC transmission lines are very important to UHV AC project construction in China.

To investigate the corona characteristic of UHV AC transmission lines, the State Grid Corporation of China built a corona cage in Wuhan UHV AC Test Base in China. The corona cage is constructed as a two-layer wire-mesh enclosure, with a cross-section of 8×8 m^2 and an effective length of 35 m. The general view and structure diagram of the corona cage are shown in Fig. 1.

Corona cage is an important apparatus for the research on the RI level of transmission lines. In the early days, there were a lot of studies on RI characteristic using corona cage. Adams [2] described the mechanism of RI field travelling along the lines and interfering with radio reception, in which the RI field was assumed a quasi-transverse electromagnetic mode (TEM) wave propagation, and the RI generation function was proposed for the first time. Then, Juette and Zaffanella [3] carried out some experiments to study the RI level using corona cage in heavy rain condition, the test results exhibited good reproducibility, and they found that the most effective way to meet the radio noise (RN) requirements of UHV was to increase the number of subconductors much above four. Later, RN data from corona cage were translated to equivalent power lines RI level by applying the excitation function [4]. At the same time, Moreau and Gary [5] fitted the excitation function with corona cage test data, and they also discussed the relationship of RI field strength between the maximum level in heavy rain and the level in dry weather based on different surface states of conductor bundles. Trinh and Maruvada [6–8] measured the excitation function values using a high-voltage coupling capacitor between the laboratory ground and bundle conductors, and proposed an excitation function of 1 MHz, which also reached a conclusion that the RI excitation function of the multiconductor bundles having three or more conductors was essentially independent of the number of subconductors. The independence of excitation function with bundle numbers was also discussed in [9]. Urban *et al.* [10] described two measuring methods of excitation function in heavy rain condition, and also considered that the dispersion of induced currents in fair weather condition is the main reason for bad reproducibility in measuring the RI level. The measuring method and the parameters selection for measuring circuit were described in [11]. There are also some studies on the RI spectrum characteristic of single test line which is terminated with different impedances [12]. The transformation relationship of RI induced currents between long and short UHVDC transmission lines was discussed in [13]. In [14], the total RN was measured across a resistor connected between the laboratory ground and the cage, and the effects of different parameters on excitation function were discussed.

Currently, the excitation function which is recommended by CISPR is widely used to predict the RI field strength of long lines. It is noted in [15] that the CISPR formula gives the upper envelope of the values that could be obtained with the other formulas and thus gives a conservative evaluation of the excitation function, so the predicted values by CISPR formula are greater than the actual RI levels. This phenomenon is confirmed by comparing the RI performances between CISPR calculations and the statistical data in Hubei long-term station, which is under the operating 1000 kV Jindongnan–Nanyang–Jingmen UHV transmission lines. In this paper, in order to obtain a more actual description of RI level caused by transmission lines, a summary of cage measurements of the RI for a large number of conductor bundles is made, and the relevant excitation function is also proposed. Then the predicted values using this function are calculated and the comparison with long-term data is presented; the results show a good match.

2 Experimental method

2.1 Introduction of test conductors

In this paper, a large number of bundle conductors are used to measure the excitation function values under the heavy rain

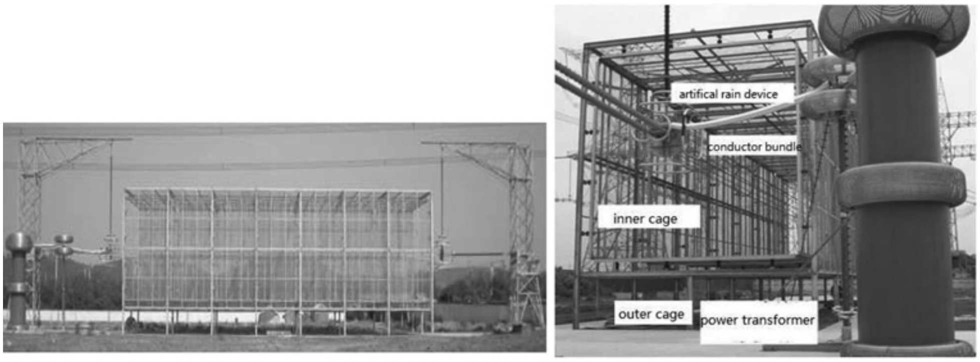

a b

Fig. 1 *UHV AC corona cage*

a General view
b Structure diagram

condition in the cage. The types of bundle conductors are given as follows: 4 × LGJ400, 4 × LGJ630, 6 × LGJ400, 6 × LGJ500, 6 × LGJ630, 8 × LGJ400, 8 × LGJ500, 8 × LGJ630, 8 × LGJ720, 8 × LGJ900, 9 × LGJ400, 9 × LGJ720, 10 × LGJ400, 10 × LGJ630, 12 × LGJ400, 12 × LGJ500, 12 × LGJ630 and 12 × LGJ720. These bundle conductors have different sizes, the subconductor diameter varies from 26.8 to 39.9 mm, whereas the bundle number alters from 4 to 12. The relationship between conductor type and subconductor diameter is shown in Table 1. Considering that the conductor spacing has negligible effect on the excitation function [7, 14], it is set to be a constant of 400 mm in this paper. The measuring frequency is 0.5 MHz, which is in accordance with direction from CISPR 18 [15], where the measurement frequency is recommended as 0.5 MHz ± 10%, and the rate of artificial heavy rain is ∼18 mm/h.

The power is supplied by a single-phase transformer with a rated voltage of 800 kV and a rated capacity of 400 kVA. The conducted RI voltage is measured by RI receiver, model FCKL 1528, from Schwarzbeck Mess Company in Germany, with the measuring error <1 dB.

2.2 Introduction of measuring method

The conducted RI voltage is measured across a resistor connected between the laboratory ground and the bundle, which requires a high-voltage coupling capacitor C_c. The schematic diagram of this method is indicated in Fig. 2, where C_c is 10 000 pF and R1 is 275 Ω.

The RI excitation function Γ is given by

$$I = \frac{C}{2\pi\varepsilon_0} \cdot \Gamma \tag{1}$$

where Γ is the excitation function value, $\mu V/\sqrt{m}$. C is the capacitance of bundle conductors in cage per unit length, I is the induced current per unit length and ε_0 is the permittivity of free space, $\varepsilon_0 = 1/36\pi \times 10^{-9}$ F/m.

The derived excitation function for a corona cage is given by

$$\Gamma_{[\mathrm{dB}\mu\mathrm{A}/\sqrt{m}]} = V_{\mathrm{RN}} + A + B + C \tag{2}$$

Table 1 Relationship between conductor type and subconductor diameter

Conductor type	LGJ400	LGJ500	LGJ630	LGJ720	LGJ900
subconductor diameter, mm	26.8	30	33.6	36.24	39.9

Unit: millimetres

where V_{RN} is the measured noise reading on meter in dBμV, and

$$\begin{aligned} A &= -20\ \lg(R) \\ B &= 20\ \lg(2\pi\varepsilon_0/C) \\ C &= -20\ \lg(\sqrt{G}) \end{aligned} \tag{3}$$

In (3), $R = (R_m + R_2)/R_m R_2$, $R_2 = R_m = 50$ Ω, G is the amplification factor caused by addition of the uniformly distributed radio-frequency currents generated on the conductor and the calculation method can be found in [6].

It should be noted that considering the size of corona cage is electrically small at a measuring frequency of 0.5 MHz, the error introduced by the mismatch between total terminal resistor and characteristic impedance of the conductor-cage system are ignored in this paper. However, the error is increased along with the increase of cage length and it cannot be ignored any more when the cage becomes more longer. Thus, when performing the measurement of the excitation function for a long cage, the total terminal resistor cannot be fixed at 300 Ω but should be matched with the characteristic impedance.

3 RI performance of bundle conductors

On the basis of test data from the corona cage, the excitation function (4) is fitted using the least mean squared error method. The formula is a function related with the average maximum bundle gradient, the subconductor radius and the number of subconductors

$$\Gamma = 55 - 576.5/g_{\max} + 42.4\ \lg(2r) - 0.714\ \lg(n) \tag{4}$$

where Γ is the excitation function value in dB(μA/m$^{1/2}$), $g_{\max}$ is the average of the maximum gradients of the individual subconductors in kilovolts/centimetres (kV/cm), r is the radii of the subconductor in centimetres and n is the number of the subconductors in the bundle.

The experimental results are all illustrated in Fig. 3. The curves represent the fitting results from (4), whereas the dots represent the measured excitation function values which have the same parameters with the fitting ones.

As shown in Fig. 3, the fitting results from (4) have a better consistency with the measured data. Besides, with the increase of subconductor diameter from 26.8 to 39.9 mm, the excitation function value of 8-conductor bundles which is widely used in UHV project is increased by 7.3 dB with the same conductor surface gradient.

IET Sci. Meas. Technol., 2015, Vol. 9, Iss. 5, pp. 621–627

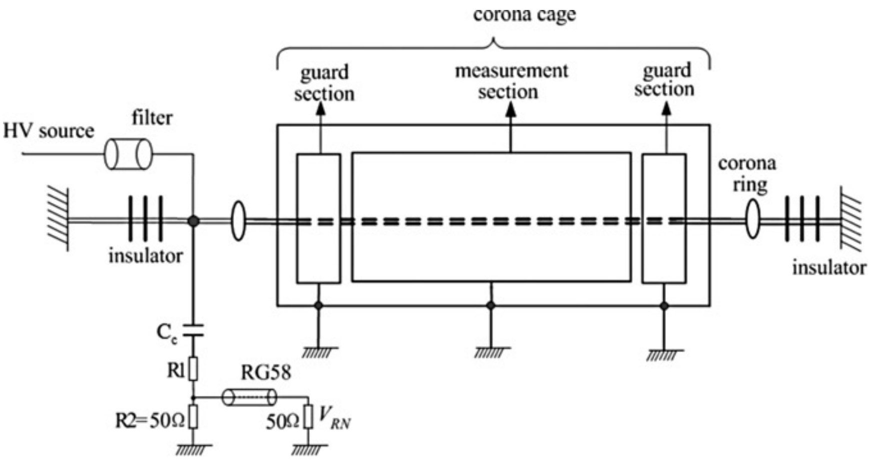

Fig. 2 *Cage setups for measuring excitation function with measuring circuit*

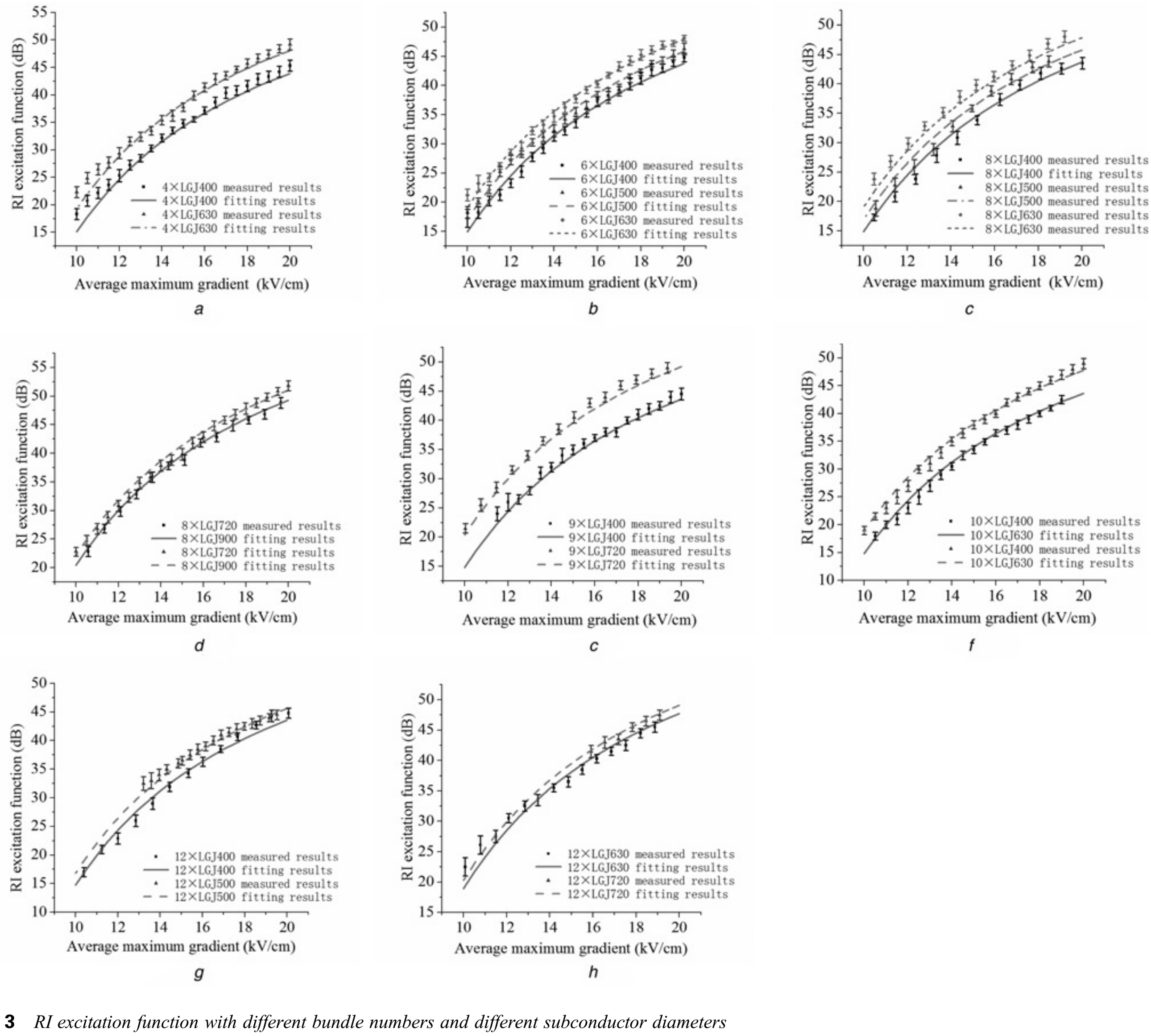

Fig. 3 *RI excitation function with different bundle numbers and different subconductor diameters*

a Four-conductor bundle
b Six-conductor bundle
c Eight-conductor bundle (No. 1)
d Eight-conductor bundle (No. 2)
e Nine-conductor bundle
f Ten-conductor bundle
g Twelve-conductor bundle (No. 1)
h Twelve-conductor bundle (No. 2)

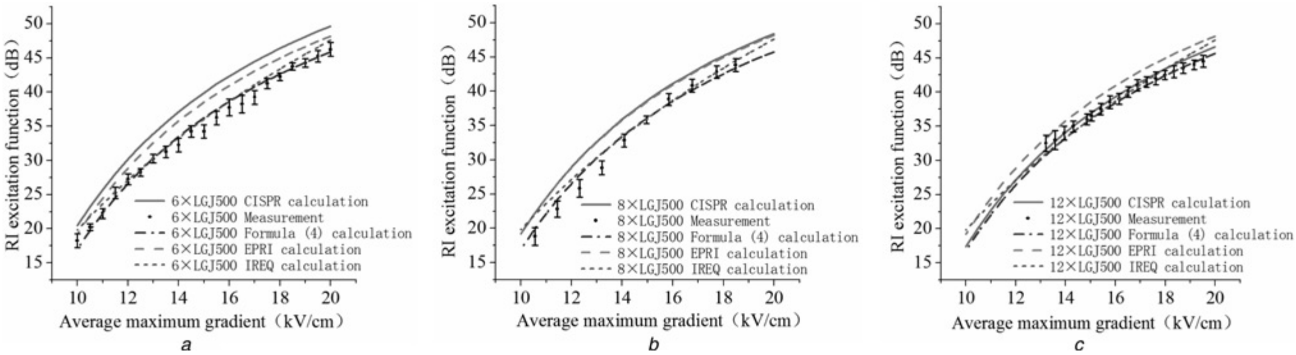

Fig. 4 *Comparison of test results and calculated results from different excitation functions*

a Contrast results of bundle conductor 6 × LGJ500
b Contrast results of bundle conductor 8 × LGJ500
c Contrast results of bundle conductor 12 × LGJ500

4 Comparison between predicted values and measured data

4.1 Comparative analysis of other organisations' excitation functions and (4)

The comparison of the test and the excitation function values from different research organisations, such as CISPR, EPRI and Hydro-Québec Research Institute (IREQ), is made for conductor LGJ500 with different bundle numbers 6, 8, 12. The results are shown in Fig. 4. These formulas are converted into CISPR measurement, assuming the measuring frequency is 0.5 MHz and the altitude is 0 m above sea level [15–17].

In Fig. 4, as the bundle number increases, the difference between the CISPR calculation and the test results become smaller. However, the deviation is very obvious for the case of bundle number 6 and 8. In general, the EPRI predictions are more than test results. It also can be found that the IREQ results are very close to (4) results and test results when the average maximum bundle gradient is between 12 and 18 kV/cm. When more than 18 kV/cm, IREQ results are slightly larger than test results. The similar characteristics are also found in conductor LGJ400, LGJ630 and LGJ720 [18].

4.2 Comparison between predicted values and long-term data

To perform further research on the RI level of UHV AC transmission lines, the Hubei long-term station was built under the operating 1000 kV Jindongnan–Nanyang–Jingmen power lines by China Electric Power Research Institute. A large number of measured data are obtained in 2011 [19]. The general view of long-term station is shown in Fig. 5, and the structure diagram of 1000 kV power lines near the Hubei long-term station is depicted in Fig. 6.

The schematic diagram of the measuring system in Hubei long-term station is shown in Fig. 7, and the instrumentation systems are described in the following.

4.2.1 Instrumentation systems: *RI receiver:* One RI receiver from Schwarzbeck Mess Elektronik (Germany), model FCKL 1528, was used to monitor the quasi-peak level of the RI, with frequency range from 9 kHz to 30 MHz, dynamic range 120 dB and the measuring error <1 dB. A PC-controlled measurement was performed, using a standard PC, an IEEE-card and the Schwarzbeck software together with the receiver.

RI antenna: One active loop antenna from ETS-Lindgren Company (USA), model 6502, was used to measure the RI field, with frequency range from 10 kHz to 30 MHz, dynamic range 125 dB and the accuracy ±1 dB. Both receiver and antenna conform to the CISPR specifications [15].

Meteorology: One weather station from Onset Computer Corporation (USA), model HOBO U30, was used to measure the meteorological parameters in the test site, including precipitation, air temperature, relative humidity, wind speed, wind direction and barometric pressure. This station consists of meteorological sensors and data logging system.

Precipitation is very important in long-term RI measurement, and was measured by HOBO rain gauge smart sensor, which is a tipping bucket. The sensor produces one tip for each 0.2 mm accumulation of water. The measured precipitation over 1 min is translated into rainfall rate, millimetres/hours. The resolution of

Fig. 5 *Long-term station in Hubei Province*

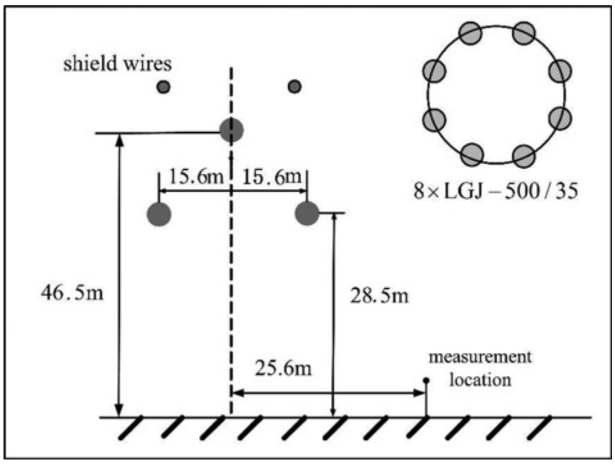

Fig. 6 *Structure diagram of power lines near Hubei long-term station*

IET Sci. Meas. Technol., 2015, Vol. 9, Iss. 5, pp. 621–627

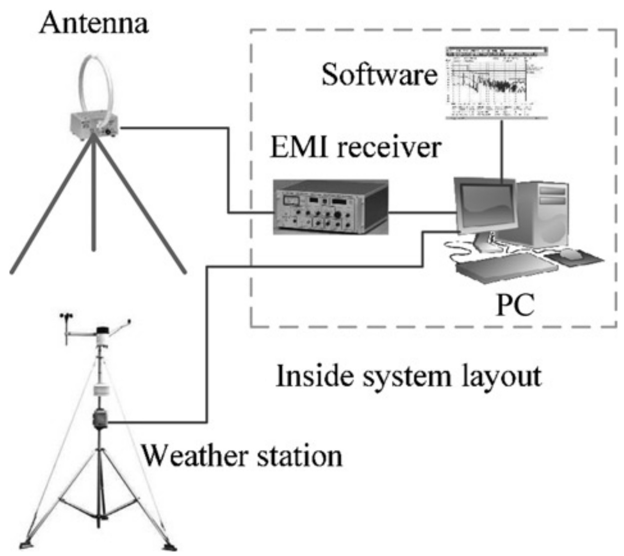

Fig. 7 *Schematic diagram of measuring system*

this sensor is 0.2 mm, with measurement range 100 mm/h and calibration accuracy ±1%.

4.2.2 Test and analysis: In this paper, the section profile distribution of RI level near Hubei long-term station is calculated by (4) with the parameters of the power lines. Then, the calculated values are compared with the statistical data. Besides, the RI level calculated by CISPR excitation function is also presented.

In the calculation, the applied voltage is 1050 kV, which is coincided with the operating voltage of this 1000 kV project in most of the time. The soil resistivity is 100 Ωm, which is obtained from grounding designer who measured the average value of soil resistivity of this place. The bundle conductor is 8 × LGJ-500/35 with bundle spacing 400 mm.

The comparison of the RI section profile distribution calculated by these two functions is illustrated in Fig. 8.

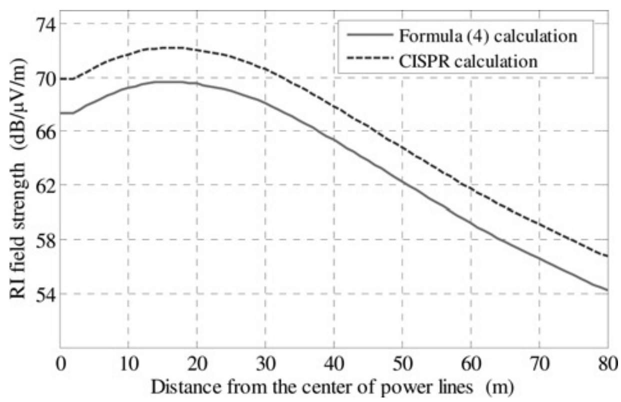

Fig. 8 *Section profile of RI distribution calculated using CISPR excitation function and (4) in Hubei Station*

Table 2 Calculated RI level outside 20 m from outer phase in heavy rain condition

Excitation function type	CISPR	Formula (4)
RI field strength, dB/μV/m	69	66.5

Unit: decibel-microvolts per meter (dB (μV/m))

Table 3 Steady RI statistic data of 20 min long outside 20 m from outer phase in heavy rain condition in Hubei Station

Sample statistics	Mean	Median	Standard deviation	Percentiles		
				50%	80%	90%
300	65.4	65.3	0.4	65.3	65.6	65.8

Unit: dB (μV/m)

It can be seen that, the calculated values of (4) are smaller than those of CISPR formula, with a difference of 2.5 dB outside 20 m from outer phase, as shown in Table 2.

The steady RI field strength of 1000 kV Jindongnan–Nanyang–Jingmen power lines outside 20 m from outer phase in heavy rain condition is obtained in Hubei Station on 18 June 2011. The average rainfall during measuring period is about 12 mm/h, and the short-time rainfall is 0.6 mm/min. The statistical results are reported in Table 3.

From Table 3, the mean of statistic data is 65.4 dB, which is 3.6 dB smaller than the calculated value from CISPR and 1.1 dB smaller than the one from (4).

Besides, the average RI levels of (4) and CISPR in fair weather condition are obtained by subtracting 20 dB from the heavy rain condition [15], which is shown in Table 4. Then the statistic data in fair weather condition obtained from Hubei long-term station in 2011 are shown in Table 5.

From Table 5, it can be seen that the mean of statistic data in Hubei Station is 47.8 dB, which is 1.2 dB lower than CISPR calculated value, while, 1.3 dB higher than calculated value from (4).

The statistic data under foul weather condition including rain and dense fog obtained from Hubei long-term station are also shown in Table 6, while the cumulative probability distributions obtained in the same station for fair, foul weather and all weathers are given in Fig. 9.

From the all-weather distribution curve in Fig. 9, the 50, 80 and 90% levels are 47, 53.1 and 58.6 dB, respectively. The difference

Table 4 Calculated RI level outside 20 m from outer phase in fair weather condition

Excitation function type	CISPR	Formula (4)
RI field strength, dB/μV/m	49	46.5

Unit: dB (μV/m)

Table 5 RI statistic data outside 20 m from outer phase in fair weather condition in Hubei Station from June to August in 2011

Sample statistics	Mean	Median	Standard deviation	Percentiles		
				50%	80%	90%
48 437	47.8	46.4	4.3	46.4	51.6	54.4

Unit: dB(μV/m)

Table 6 RI statistic data outside 20 m from outer phase in foul weather condition in Hubei Station from June to August in 2011

Sample statistics	Mean	Median	Standard deviation	Percentiles		
				50%	80%	90%
5194	56.3	56.7	5.2	56.7	61	62.7

Unit: dB(μV/m)

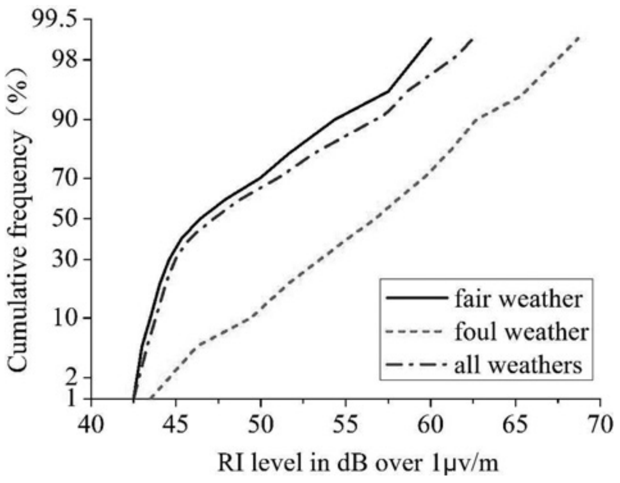

Fig. 9 *Statistical distribution of RI level at Hubei Station in fair, foul weather and all weathers from June to August in 2011*

between the 95 and 80% levels is 5.5 dB, which lies between 5 and 12 dB summarised in CISPR18 [15].

In summary, the 50% fair weather level is 46.4 dB, 80% all-weather level is 53.1 dB and 50% heavy rain level is 65.3 dB. The difference between 80% all-weather level and 50% fair weather level is 6.7 dB, the difference between 50% heavy rain level and 80% all-weather level is 12.2 dB and the difference between 50% heavy rain level and 50% fair weather level is 18.9 dB. These differences are within the range of [5 dB, 15 dB], [5 dB, 15 dB] and [16 dB, 25 dB], respectively, which are summarised in CISPR18 [15]. Obviously, the statistic data in Hubei Station are in coincidence with the statistic laws in CISPR18.

In addition, because of the small quantity of valid stable RI data in heavy rain condition in Hubei Station, the long-term RI levels of second-generation 735 kV power lines recorded by IREQ (Hydro-Québec's research institute) in stable heavy rain condition in Canada, are used to verify (4) [16, 20].

The basic parameters of second-generation design of Hydro-Québec's 735 kV power lines are shown in Fig. 10. The antenna height is 1 m, and the earth resistivity is 250 Ωm. Then the section profile of 0.5 MHz RI distribution is calculated, and the results are shown in Fig. 11. The CISPR value and (4) value are calculated as 77.9 and 72.5 dB, respectively, with a distance of 28.7 m away from the centre lines. The statistical stable RI level by IREQ in heavy rain condition is 68 dB using American National Standards Institute (ANSI) receiver with a frequency of 1 MHz [16]. When replacing ANSI receiver with a CISPR one (−2 dB), and changing the frequency from 1 to 0.5 MHz (+5.1 dB), the stable RI level turns to be 71.1 dB [16], which is 6.8 dB smaller than the theoretical value of CISPR and 1.4 dB smaller than the one from (4).

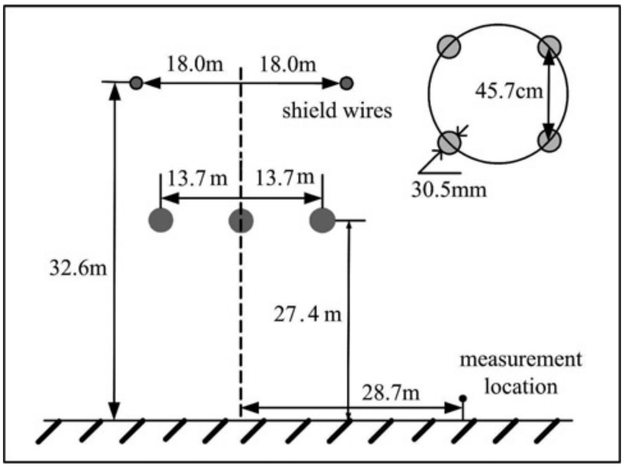

Fig. 10 *Structure diagram of second-generation design of Hydro-Québec's 735 kV power lines*

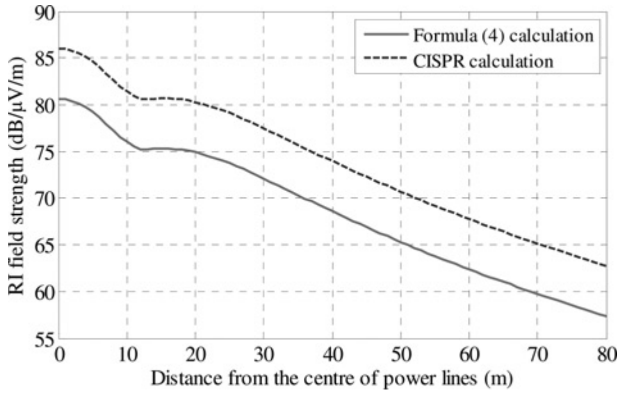

Fig. 11 *Section profile of RI distribution calculated about Hydro-Québec's 735 kV power lines*

4.2 Discussion of CISPR formula and (4)

Although (4) can make a more actual assessment about the excitation function values and RI levels in heavy rain condition than CISPR formula from the above analysis, the CISPR formula is still indispensable in evaluating the RI performance for the reason that it can provide a conservative reference value for a rigorous evaluation. Therefore in order to ensure the RI level of a pre-design power lines do not exceed the standard, meanwhile, this level is not overly conservative which can lead to a substantial increase in construction costs, (4) and CISPR formula should be combined together for a comprehensive evaluation.

5 Conclusion

(1) Using the experimental results in corona cage, a useful excitation function is fitted in heavy rain condition.
(2) Considering the same conductor surface gradient, the excitation function of 8-conductor bundles increases by 7.3 dB with the subconductor diameter changing from 26.8 to 39.9 mm.
(3) The RI calculated values of (4) are compared with the long-term data from Hubei station and IREQ, and the result shows a good agreement.
(4) The long-term data in Hubei Station are in coincidence with the conversion laws of RI at different weather conditions proposed in CISPR18, which means that these laws are also applicable to 1000 kV UHV transmission lines.

6 References

1 Urban, R.G.: 'Power line corona prediction from small cage measurement'. PhD dissertation, Department of Electrical Electronic Engineering, Stellenbosch University, Stellenbosch, South Africa, 2004
2 Adams, G.E.: 'The calculation of the radio interference level of transmission lines caused by corona discharges', *IEEE Trans. Power Appar. Syst.*, 1956, **75**, (3), pp. 411–419
3 Juette, G.W., Zaffanella, L.E.: 'Radio noise, audible noise, and corona loss of EHV and UHV transmission lines under rain: predetermination based on cage tests', *IEEE Trans. Power Appar. Syst.*, 1970, **89**, (6), pp. 1168–1178
4 Gary, C.H.: 'The theory of excitation function: a demonstration of its physical meaning', *IEEE Trans. Power Appar. Syst.*, 1972, **91**, (1), pp. 305–310
5 Moreau, M.R., Gary, C.H.: 'Predetermination of the radio interference level of high voltage transmission lines I: predetermination of the excitation function', *IEEE Trans. Power Appar. Syst.*, 1972, **91**, (1), pp. 284–291
6 Trinh, N.G., Maruvada, P.S.: 'A comparative study of the corona performance of conductor bundles for 1200 kV transmission lines', *IEEE Trans. Power Appar. Syst.*, 1974, **93**, (3), pp. 940–949
7 Trinh, N.G., Maruvada, P.S.: 'A method of predicting the corona performance of conductor bundles based on cage test results', *IEEE Trans. Power Appar. Syst.*, 1977, **96**, (1), pp. 312–325

8 Maruvada, P.S.: 'Corona performance of high-voltage transmission lines' (Research Studies Press, Baldock, UK, 2000)
9 Alexandrov, A.: 'EHV equipment and its surrounding environment protection' (Chongqing University Press, Chongqing, China, 1996)
10 Urban, R.G., Reader, H.C., Holtzhausen, J.P.: 'Small corona cage for wideband HVac radio noise studies: rational and critical design', *IEEE Trans. Power Deliv.*, 2008, **23**, (2), pp. 1150–1157
11 Begamudre, R.D.: 'Extra high voltage AC transmission engineering' (New Age International Press, New Delhi, India, 2008, 3rd edn.)
12 Yang, B., Zhang, B.: 'Simulation analysis of effectiveness of radio interference measurement on test line', *(Chin.) High Volt. Eng.*, 2011, **37**, (12), pp. 2978–2983
13 Xie, L., Lu, J.J., Zhang, W.L., Guo, J.: 'Analysis on radio interference transformation relation between long and short UHVDC transmission lines'. (in Chinese) Proc. of the CSEE, 2013, vol. 33, no. 7, pp. 109–115
14 Tang, J.: 'Study on corona effects and electromagnetic environment of 1000 kV ultra-high voltage AC transmission line'. PhD dissertation, Department of Electrical and Engineering, Tsinghua University, 2009
15 Radio interference characteristics of overhead power lines and high-voltage equipment (2nd edn.), CISPR Standard 18, June 2010
16 Olsen, R.G., Schennum, S.D., Chariter, V.L.: 'Comparison of several methods for calculating power line electromagnetic interference levels and calibration with long-term data', *IEEE Trans. Power Deliv.*, 1992, **7**, (2), pp. 903–913
17 Comber, M.G., Nigbor, R.J.: 'Transmission line reference book: 345 kV and above' (Fred Weidner & Son Printers, INC, USA, 1982)
18 Wan, B.Q., Chun, C.M., Chen, Y.C., He, W.L.: 'Study on corona performance of conductor bundles based on corona cage'. Technical Report, SG1021, (in Chinese) China Electric Power Research Institute, Wuhan, China, August 2013
19 Wu, X., Wan, B.Q., Zhang, Y.M.: '1000 kV Jindongnan–Nanyang–Jingmen UHV AC project: the long-term measurement of the project electromagnetic environment level'. Technical Report, SGTGY (2009) 681, (in Chinese) China Electric Power Research Institute, Wuhan, China, November 2011
20 Trinh, N.G., Maruvada, P.S., Flamand, J., Volotrire, J.R.: 'A study of the corona performance of hydro Quebec's 735 kV lines', *IEEE Trans. Power Appar. Syst.*, 1982, **101**, (3), pp. 691–690